

pubs.acs.org/JPCL Letter

Density-Corrected Density Functional Theory for Open Shells: How to Deal with Spin Contamination

Hayoung Yu, Suhwan Song, Seungsoo Nam, Kieron Burke, and Eunji Sim*



Cite This: J. Phys. Chem. Lett. 2023, 14, 9230-9237



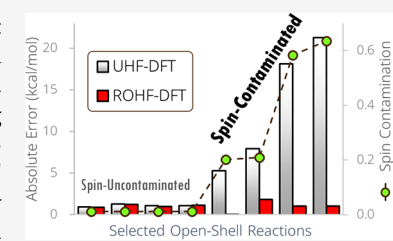
ACCESS

III Metrics & More

Article Recommendations

Supporting Information

ABSTRACT: Density functional theory (DFT) is usually used self-consistently to predict chemical properties, but the use of the Hartree–Fock (HF) density improves energetics in certain, well-characterized cases. Density-corrected (DC) DFT provides the theory behind this, but unrestricted Hartree–Fock (UHF) densities yield poor energetics in cases of strong spin contamination. Here we compare with restricted open-shell HF (ROHF) across 13 different functionals and two DC-DFT methods. For significant spin contamination, ROHF densities outperform UHF densities by as much as a factor of 3, depending on the energy functional, and ROHF-DFT improves over self-consistent DFT for most of the tested functionals. We refine the DC(HF)-DFT algorithm to use ROHF densities in cases of severe spin contamination.



ensity functional theory (DFT) is a method for calculating the properties of electronic systems using electron density as the basic variable. Given the exact exchange—correlation functional, the exact density is found in the Kohn—Sham (KS) equations and exact energies and associated properties can be extracted. In practical calculations, the exact energy functional is unknown and DFT is performed with approximate density functionals. The self-consistent solutions of the KS equations therefore yield approximate densities. In most practical DFT calculations, the error in the approximate density is negligible and can be safely ignored.

Density-corrected DFT (DC-DFT)¹ provides a theoretical framework with which to analyze the origin of errors in any DFT calculation.^{2,3} DC-DFT unambiguously separates the energy error into the error due to the functional and the error due to the density. In most DFT calculations, the density-driven error is negligible, but in certain well-characterized cases, the density-driven error dominates. Use of a more accurate density then greatly reduces the overall error. In many cases of typical large density-driven errors, the HF density suffices, as has been explicitly demonstrated for stretched NaCl and HO·Cl⁻ radicals.⁴

The method HF-DFT uses HF densities instead of self-consistent ones in *every* DFT calculation and has emerged as an extremely useful practical procedure. The cases where HF-DFT showed remarkable success include pure water and aqueous systems, ^{6–8} electron and hole polaron defects, ⁹ crystal polymer conformational energies, ¹⁰ making and breaking of internal hydrogen bonds, ¹¹ torsional barriers, ¹² electron affinity, ¹³ dissociation energy curves of heteronuclear molecules, ^{4,14} radical ions in aqueous solution, ¹⁵ spin gaps of Fe(II) complexes, ¹⁶ halogen and chalcogen binding energies, ¹⁷ etc. HF-DFT not only works for the energetics but also provides

sufficient accuracy similar to self-consistent DFT in various molecular properties. ¹⁸

On the other hand, the more nuanced DC(HF)-DFT *only* employs HF densities when density-driven errors are believed to be large. This more nuanced approach is vital in several important ways: (a) in finding significant improvements due to HF densities in large data sets, where the vast majority of the data does not have significant density-driven errors;² (b) in isolating improved parameters in empirical functional construction by fitting only to functional errors, not density-driven ones;¹⁹ and (c) in improving the coefficients in empirical corrections to dispersion corrections, which can be corrupted when density-driven errors are large.⁸

However, in many cases with significant density-driven errors, HF solutions break the spin symmetry. In some cases, the spin symmetry-breaking is irrelevant, but in others, significant spin-contamination of the unrestricted HF (UHF) wave function results. In those cases, the present DC-DFT procedure is to revert to the self-consistent density, as the UHF density is unlikely to be accurate for spin-contaminated cases. ^{2,20} Many chemically interesting systems are open-shell and subject to UHF spin contamination. ²¹ For example, conjugated radicals such as biradicals, ²² phenolic antioxidants included in plant foods such as anthocyanins found in berries, ^{23,24} or reactive radical species involved in atmospheric chemistry such as acetylperoxy radical. ²⁵ We examine that for

Received: July 20, 2023 Accepted: October 2, 2023 Published: October 9, 2023





many functionals (not all), when spin contamination is significant, there is a dramatic improvement in DC-DFT if restricted open-shell HF (ROHF) is used instead of UHF, presumably (but not definitively) because the ROHF wave function yields more accurate spin densities than UHF, as measured energetically by DC-DFT. On the other hand, if spin contamination is small or zero, there is little difference between using ROHF and UHF densities. Therefore, one can safely use ROHF in all DC-DFT calculations, ignoring concerns about spin contamination. This greatly extends the applicability of DC-DFT to those many chemically interesting problems mentioned above.

Background. DC-DFT emphasizes several important points to be considered when designing approximate functionals and analyzing their performance. The total error ΔE in any self-consistent DFT calculation can be written as

$$\Delta E = \tilde{E}[\tilde{n}] - E[n] = \Delta E_{F} + \Delta E_{D} \tag{1}$$

where E[] is the exact total energy functional and n is the exact electron density for the given system, while the tilde indicates their approximate counterparts. This total error can be split into two parts: the functional error $(\Delta E_{\rm F})$ and the density-driven error $(\Delta E_{\rm D})$

$$\Delta E_{\rm F} = \tilde{E}[n] - E[n]$$

$$\Delta E_{\rm D} = \Delta E - \Delta E_{\rm F} = \tilde{E}[\tilde{n}] - \tilde{E}[n]$$
 (2)

In DC-DFT, correcting the density means reducing the density-driven error by calculating the DFA energy at a more accurate density. As the exact density $n(\mathbf{r})$ is not available in practical calculations, very often the HF density is used in its place.

In most DFT calculations, the error is dominated by the functional contribution. But in many well-characterized situations, the density-driven error can be unusually large (called "abnormal" calculations), and use of the exact density significantly reduces the total error. The abnormality of a given calculation depends on the property, system, and DFA being used. Moreover, if a calculation is normal, removal of the density-driven error might even slightly worsen results.

To determine when one should throw out the self-consistent density, the concept of density sensitivity (\tilde{S}) was introduced, which is practically quantifiable as¹⁷

$$\tilde{S} = |\tilde{E}[n^{LDA}] - \tilde{E}[n^{HF}]| \tag{3}$$

where \tilde{E} is the DFA of interest and n^{LDA} and n^{HF} are the electron densities obtained by LDA and HF, respectively. A density sensitivity over 2 kcal/mol provides a practical guide for when self-consistent densities are likely problematic. ^{8,17,26} This generic rule works well for covalent bonds in small molecules but must be modified for weaker bonds or bigger molecules. Other metrics to evaluate density sensitivity have been proposed, ^{27,28} and a suitable method for the context should be chosen.

The energy of a density-sensitive calculation tends to vary a lot depending on different density inputs, and small density errors may cause large density-driven errors. In DC(HF)-DFT, we replace the self-consistent density with the HF density only in density-sensitive cases, which has proven very successful. On the other hand, HF-DFT is the indiscriminate use of the HF density in all cases, regardless of density sensitivity, but since density-insensitive cases greatly outnumber density-sensitive cases in large databases, such as

GMTKN55, a small (and unimportant) increase in errors from using the HF density when inappropriate can easily mask the large (and significant) improvement due to the HF density in density-sensitive cases.^{2,11}

Next we turn to spin contamination in UHF calculations, which means that the wave function is contaminated by higher spin states, instead of representing a desired single spin state. The amount of spin contamination $\Delta \langle \hat{S}^2 \rangle$ can be practically measured by the deviation of the spin expectation value from the exact value that should come out from a wave function of a pure spin state: 30

$$\Delta \langle \hat{S}^2 \rangle = \langle \hat{S}^2 \rangle - S_z (S_z + 1) \tag{4}$$

Spin contamination can appear and be evaluated in many open-shell quantum chemistry methods, such as in HF, DFT, second-order Møller-Plesset perturbation theory (MP2), coupled-cluster singles and doubles (CCSD), etc.^{29,31,32} Post-HF or double-hybrid density functional calculations using a spin-contaminated UHF wave function can yield very poor results.³¹ Previously, it was demonstrated that replacing UHF with ROHF in WFT-in-DFT embedding led to improved accuracy by mitigating spin contamination,³³ and there has also been an attempt to suppress spin contamination in hydrogenatom transfer reactions using ROCBS-QB3 and ROCCSD.³⁴ In the present work, we investigate whether a similar enhancement can be achieved within the context of HF-DFT. However, the unrestricted scheme is the most frequently used open-shell method in both HF and DFT. Its simple definition and ease of computation make the unrestricted scheme highly desirable. Unrestricted Kohn-Sham wave functions are less likely to be spin-contaminated than their HF counterparts, 20,35 which has led to less attention to the problem of spin contamination in DFT.

It is important to distinguish our use of ROHF from those traditionally used in wave function calculations or in DFT. For a wave function method starting from an HF calculation, spin contamination of the starting point can lead to severe inaccuracies in any wave function built upon it.30 Since a perfect method would be independent of the starting point but imperfect methods are not, significant improvement in the quality of the wave function can be achieved by removing spin contamination. On the other hand, there are strong arguments against removing spin contamination in DFT calculations, especially for materials. ^{36–38} For approximate functionals, a broken spin-symmetry solution will typically yield the best energetics, and even broken-symmetry densities can capture frozen fluctuations of the true ground state. Neither of these cases applies here, as we are simply asking which HF densities yield the best energies when approximate density functionals are applied to them (and none are self-consistent).

Many ROHF schemes or spin-projected UHF schemes have been suggested to deal with the problem, which perfectly or partially remove the spin contamination through various means. A weakness of ROHF is that it is not a uniquely defined method nor does it provide a single set of orbitals. This leads to difficulty in analyzing the orbital energies or defining perturbation methods based on ROHF orbitals.³⁹ There exist studies comparing orbital energies or total energies of different open-shell HF schemes,³¹ but there have been no studies comparing the densities or their effect on HF-DFT energies. Here we focus on the influence of spin-contaminated UHF density versus spin-pure ROHF density on HF-DFT

calculations and compare the results. We call them UHF-DFT and ROHF-DFT, respectively.

ROHF in DC-DFT. We need a uniquely defined ROHF scheme that differs from UHF mainly in the case of spin contamination. There exist many combinations of ROHF coefficients⁴⁰ or projected UHF schemes.^{31,41-43} We have chosen the constrained-UHF (CUHF) algorithm, which employs parameter-free Fock matrices to mathematically constrain the spin density eigenvalues of UHF. This approach yields orbital energies that retain their physical significance similar to UHF, while effectively eliminating spin contamination.⁴³ The scope of CUHF can be extended as a bridge between ROHF and UHF by widening the active space of the orbitals, and MP2 utilizing CUHF orbitals (CUMP2) is also available. 44 Comparing results by varying the range of active spaces could provide a more sophisticated study of the effect of spin contamination, but here, we have implemented the CUHF algorithm simply as an ROHF scheme. We denote these methods as ROHF and ROMP2 in what follows. Figure 1

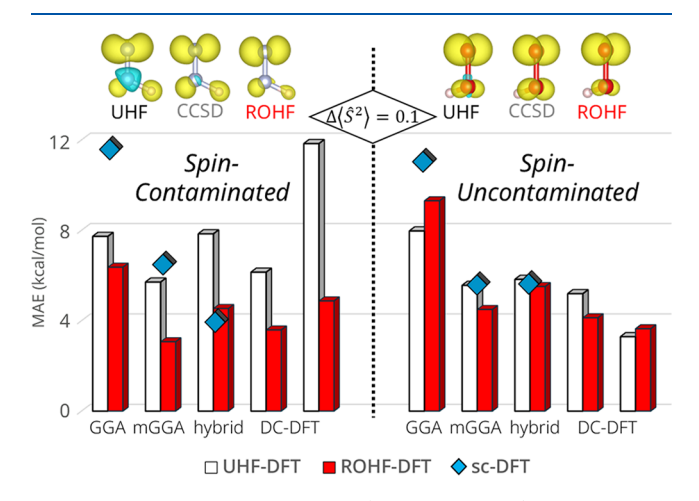


Figure 1. Mean absolute errors (MAE, kcal/mol) of open-shell subsets of GMTKN55 database using various self-consistent (sc-)/UHF-/ROHF-DFT methods. Spin-contaminated cases are on the left, and spin-uncontaminated cases are on the right. The plotted functionals are PBE (GGA), r²SCAN (mGGA), PBE0 (hybrid), HF-r²SCAN-DC4, and BL1p (DC-DFT). Top: Spin density plot examples for UHF, ROHF, and CCSD of molecules HNN (left) and HOO (right).

summarizes our results. It shows that for many functionals (not all), there is little difference between ROHF and UHF if spin contamination is small or zero (right-hand side). However, in the presence of spin contamination (left-hand side), there is a dramatic improvement, with the largest improvement being for functionals designed with DC-DFT principles, i.e., functionals whose energetics are trained with density-driven errors removed.

It is important to note that the ROHF wave function may have lost some other features in return for the exact spin eigenvalue, and other errors may be inherent in its density. However, Figure 1 and further discussion below show that, at least when spin contamination in UHF is severe, simply replacing by ROHF can effectively reduce the errors in UHF-DFT induced by spin contamination. We will define every open-shell system as spin-uncontaminated or spin-contaminated and compare the performance of UHF- and ROHF-DFT in each. Typically, a UHF wave function with $\Delta \langle \hat{S}^2 \rangle$ over 0.1^{30}

or $10\%^{45}$ is considered severely spin-contaminated. The former criterion works well for this study, so we distinguish spin contamination by $\Delta \langle \hat{S}^2 \rangle > 0.1$ (see Figure S1).

Before we continue with the results, we must sound a note of caution. The spin density plots of UHF and ROHF in Figure 1 are provided simply to convey the concept. In fact, in most interesting cases, we find it impossible to decide which is a "better" density by simple inspection of such plots. "Correcting" the density in DC-DFT means reducing the density-driven error, but this does not directly translate into a visually favorable density. Very tiny features in densities can yield significant differences in energies. Two densities may appear remarkably similar but have substantially different exchange-correlation energies with a given functional. On the other hand, densities that differ significantly in some region might have almost identical energies. Moreover, which is dependent on the functional being applied. Thus, within DC-DFT, contour plots of densities and density differences, while useful, can never substitute for the accurate calculation of density-driven errors.

Here, we study simply the effect of using either HF density on open-shell cases. Of the 1505 numbers in the GMTKN55 database, about 30% (430 cases) contain an open-shell species. Of these, about 10% (46 cases) are spin-contaminated. Table 1 gives results for 13 different functional approximations, comparing errors when self-consistent UHF and ROHF densities are used. Four functionals indicated by footnote "b" are the best-performing functional in each rung (GGA/mGGA/hybrid/double-hybrid) among the ones assessed in ref 46, and their self-consistent results are given for comparison.

We compare the performance by the weighted total mean absolute deviation (WTMAD-2), proposed together with the GMTKN55 database, 46 instead of the conventionally used mean absolute errors (MAEs). WTMAD-2 compares errors in different subsets by giving weights depending on their reference energies (see the Supporting Information for the definition). Using this weighted scheme, small relative energies such as weak noncovalent interactions have more influence on the performance.

For spin-contaminated reactions, use of the ROHF density yields better energetics than the UHF density for *every* functional listed. The errors are reduced by at least 30% and sometimes up to 70%. There are a few cases where ROHF density worsens the energetics. For instance, ROHF-r²SCAN-DC4 worsens the energetics of 6 out of 46 spin-contaminated cases by more than 2 kcal/mol compared to their UHF counterparts (see the Supporting Information). We speculate that such cases might involve multireference character.

Comparing self-consistent versus ROHF densities on spin-contaminated cases, ROHF densities reduce the errors for most of the functionals but not for BLYP and M06-2X. For BLYP, the difference is about 1 kcal/mol of WTMAD-2, and for M06-2X, it is about 4.5 kcal/mol. The behavior of HF densities on Minnesota functionals and hybrids is not expected to be consistent because they are empirically fitted to reduce the total error without separating the density-driven errors from functional errors. The ROHF-DFT method even outperforms the four functionals, chosen in ref 46 as the best-performing functional on the GMTKN55 database in each rung.

The last two lines of Table 1 are designed to test ROHF for two DC functionals, i.e., functionals designed to be used on

Table 1. Weighted Total Mean Absolute Deviations (WTMAD-2, kcal/mol) Are Calculated for the Spin-Contaminated (SC) and Spin-Uncontaminated (SU) Reactions Using Various Self-Consistent (sc-)/UHF-/ROHF-DFT Methods^a

		SC (46)			SU (384)		
		SC-	UHF-	ROHF-	sc-	UHF-	ROHF
GGA	BLYP	7.60	19.36	8.69	7.72	5.98	6.85
	PBE	16.65	16.65	7.23	9.89	5.20	6.13
	PW91	16.74	15.96	7.13	10.17	5.24	6.13
	PRBE	13.83	18.44	6.70	8.23	5.28	5.98
	RevPBE-D3(BJ) ^b	14.44			8.14		
MGGA	M06-L	13.72	14.47	8.09	6.63	5.12	5.54
	TPSS	14.67	15.04	6.54	8.22	5.54	5.71
	SCAN	14.00	7.32	4.78	6.97	4.54	4.09
	r ² SCAN	12.40	8.84	4.49	6.70	4.42	4.23
	SCAN-D3(BJ) ^b	14.18			7.01		
Hybrid	B3LYP	9.96	16.66	5.77	6.53	4.96	5.09
	TPSSh	11.48	13.75	5.08	6.97	5.34	5.25
	M06	7.50	17.18	6.92	4.24	3.97	4.25
	PBE0	8.48	13.07	5.24	5.52	3.43	3.71
	M06-2X	2.67	23.44	7.12	3.34	3.14	3.53
	ω B97X-V b	5.82			1.51		
	DSD-BLYP-D3(BJ) ^b	4.97			3.51		
			DC-DFT				
	HF-r ² SCAN-DC4	12.60°	8.97	4.69	6.71 ^c	4.31	4.13
	BL1p		25.42	5.40		3.39	3.55

[&]quot;Number of reactions included in SC/SU are given in parentheses. ^bBest-performing functional in each rung among the accessed functionals in ref 46 are shown for comparison. ^cr²SCAN-D4 is calculated with Grimme's original set of parameters (see Table S1 for the D4/DC4 parameters).

HF densities; HF-r²SCAN-DC4⁸ and BL1p. 19 We denote the methods as UHF-/ROHF-r²SCAN-DC4 and UBL1p/ ROBL1p utilizing either UHF or ROHF densities. For the parametrization of two methods (DC4 in the former and α in the latter), the same values are used for both densities (see the Supporting Information for details). The main difference is that unlike HF-r²SCAN-DC4, BL1p includes MP2 energies based on the HF method used to calculate the input density. In both cases, ROHF yields much improved results for the spincontaminated set. ROHF slightly worsens the spin-uncontaminated cases for BL1p, but the effect is so small that its overall performance is still improved relative to that of UHF. Interestingly, ROHF-r²SCAN performs slightly better than ROHF-r²SCAN-DC4, for spin-contaminated cases. This could be an error cancellation due to the lack of dispersion, or because the spin-contaminated cases were not heavily considered when fitting the DC4 parameters. Either explanation would be interesting to study further. Still, ROHFr²SCAN-DC4 works better than r²SCAN-D4, which was not fitted based on DC-DFT.

How sure are we that the improvement for spin-contaminated cases is not accidental? For a more in-depth analysis, the WTMAD-2 of the original UHF-based and ROHF-based methods is compared in Figure 2, as a function of the level of spin contamination. The two HF-r²SCAN-DC4 schemes exhibit similar performance for spin-uncontaminated cases ($\Delta \langle \hat{S}^2 \rangle < 0.1$). The WTMAD-2 using the UHF density jumps tremendously when $\Delta \langle \hat{S}^2 \rangle > 0.3$, becoming much larger than that of ROHF. UBL1p and ROBL1p exhibit trends similar to those of HF-r²SCAN-DC4 but display a larger difference in the spin-contaminated region. This discrepancy can be attributed to the inclusion of MP2 in BL1p, which is even more susceptible to contamination in the wave function.

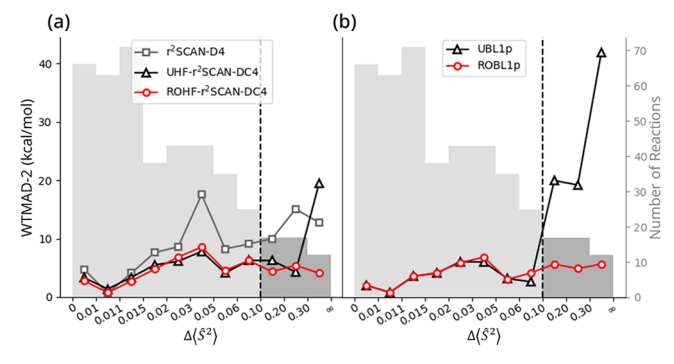


Figure 2. The weighted total mean absolute deviations (WTMAD-2, kcal/mol) for varying values of $\Delta \langle \hat{S}^2 \rangle$ in open-shell cases in GMTKN55. In panel a, r²SCAN-D4, UHF- and ROHF-r²SCAN-DC4 are plotted in gray, black and red, respectively. In panel b, UBL1p and ROBL1p are plotted in black and red, respectively. Gray bars represent the number of reactions included in the range of $\Delta \langle \hat{S}^2 \rangle$. The vertical dashed line at $\Delta \langle \hat{S}^2 \rangle = 0.1$ divides the data into two categories: spin-uncontaminated (left) and spin-contaminated (right). Note that the ranges were arbitrarily chosen to achieve a similar number of reactions within each range.

Now, we focus on some specific dramatic and chemically interesting examples. Table 2 shows the cases in RSE43, a subset of GMTKN55 consisting of radical stabilization energies. In the four highly spin-contaminated cases, UBL1p yields high errors by calculating the MP2 energy based on a highly spin-contaminated UHF wave function. Especially when $\Delta \langle \hat{S}^2 \rangle > 0.5$, the UHF error is ~20 kcal/mol, but only 1 kcal/mol in ROHF. On the other hand, the spin-uncontaminated cases show very small differences between UHF and ROHF. A similar trend occurs for HF-r²SCAN-DC4, but the failure in spin-contaminated reactions is larger in UBL1p than in UHF-

Table 2. Errors for the Extreme Reactions in RSE43^a

			BL1p		r ² SCAN-DC4	
reaction	$\Delta \langle \hat{S}^2 angle$	Ref.	UHF	ROHF	UHF	ROHF
$C_3H_3N + CH_3^* \rightarrow CH_4 + C_3H_2N^*$	0.63	2.0	21.26	1.04	7.03	-1.21
$C_7H_8 + CH_3^* \rightarrow CH_4 + C_7H_7^*$	0.58	-15.3	18.11	1.01	8.66	2.04
$C_3H^4 + CH_3^* \rightarrow CH_4 + C_3H_3^*$	0.21	-13.1	7.91	1.84	0.66	0.45
$C_3H_6 + CH_3^* \rightarrow CH_4 + C_3H_5^*$	0.20	-17.7	5.31	0.05	-0.02	-0.40
$CH_4O + CH_3^* \rightarrow CH_4 + CH_3O^*$	0.01	-4.3	0.92	0.90	-0.52	-0.48
$CH_6P^+ + CH_3^* \rightarrow CH_4 + CH_5P^*$	0.01	0.6	1.26	1.23	0.19	0.18
$C_2H_3F_3 + CH_3^* \rightarrow CH_4 + C_2H_2F_3^*$	0.01	1.4	1.07	1.00	-0.19	-0.21
$CH_3F + CH_3^* \rightarrow CH_4 + CH_2F^*$	0.01	-3.8	1.09	1.15	-0.16	-0.12

"Highest (top 4) and lowest (bottom 4) spin contamination ($\Delta \langle \hat{S}^2 \rangle$ is given). The Ref. column shows the reference reaction energies from ref 46. The four columns on the right show the errors of each method calculated by reaction energies minus reference energies in kcal/mol. Results using BL1p are also shown in the graphical abstract.

r²SCAN-DC4. Menon and Radom showed that double-hybrid functionals are less likely to be affected by spin contamination, compared to pure UHF and UMP.³² BL1p is evaluated on the HF density and includes the UMP2 energy, so the errors induced by spin contamination are larger.

Severe spin contamination in UHF might also indicate a multireference character of the system, where ROHF might not help. Here we have proposed and tested the well-known ROHF scheme as a cheap and simple solution, but there could be other alternatives that treat spin better than either UHF or ROHF. In any case, one should avoid using a highly spin-contaminated UHF wave function.

DC(HF)-DFT Avoiding Spin Contamination. Now we combine the above discussion with the DC(HF)-DFT protocol. Previously the protocol was to check the density sensitivity and decide whether to use the HF density or not. In the cases of UHF strong spin contamination, one simply reverted to the self-consistent DFT density instead.

Our ROHF results dictate an alternative. Before density sensitivity is calculated, check the UHF spin contamination. If the value is over the 0.1 criterion, UHF should be replaced by ROHF. We define \tilde{S} as \tilde{S}_U or \tilde{S}_{RO} from eq 3 using UHF and ROHF densities, respectively.

$$\tilde{S} = \begin{cases} \tilde{S}_{\text{RO}}, & \text{if spin-contaminated } (\Delta \langle \hat{S}^2 \rangle \ge 0.1) \\ \tilde{S}_{\text{U}}, & \text{otherwise } (\Delta \langle \hat{S}^2 \rangle < 0.1) \end{cases}$$
(5)

Figure 3 shows the \tilde{S} criterion scan results using three different functionals: PBE, r^2SCAN , and PBE0. Red dashed lines show the DC(HF)-DFT scheme suggested above. For DC(HF)-DFT without dispersion correction (red solid lines), local minima appear near the conventional density sensitivity criterion of 2 kcal/mol. This means that using HF densities only for density-sensitive cases (and self-consistent densities for all others) give the best results. However, addition of DC4 eliminates this minimum; that is, errors are least when HF densities are used consistently. However, as the differences are very slight, we keep the density-sensitivity criteria suggested earlier.²

Finally, after the appropriate density has been chosen, a dispersion correction should be added for the functional error correction. Dispersion corrections are vital to correctly describe noncovalent interactions or long-range interactions, and parameters should be optimized based on DC-DFT principles, so as not to spoil the dispersion correction by the density-driven error.¹⁷ For example, DC4 can be used, which is

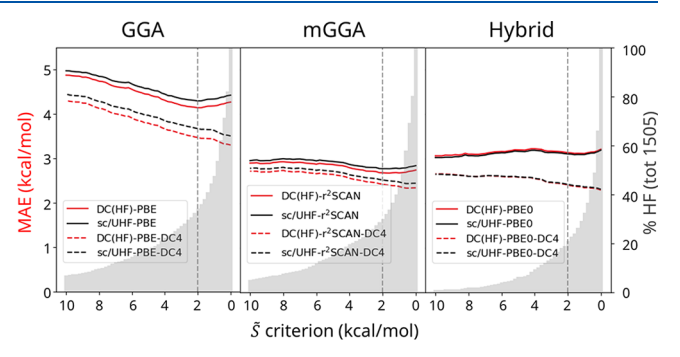


Figure 3. Density sensitivity \tilde{S} criterion scanned from 0 to 10 on GMTKN55. For a given criterion, the density is chosen between HF and self-consistent depending on whether its \tilde{S} value exceeds the criterion. The self-consistent (sc-)/UHF-DFT (black lines) uses UHF densities without considering spin contamination. In DC(HF)-DFT (red lines), ROHF density is used when UHF is spin-contaminated. Results are shown for GGA(PBE), mGGA(r²SCAN), and Hybrid-(PBE0). The vertical line represents $\tilde{S} > 2$ kcal/mol criterion. Gray bars show the percentage of HF densities chosen for each criterion.

a variation of Grimme's D4 dispersion correction⁴⁷ parametrized by Song et al.⁸ to create HF-r²SCAN-DC4.

Figure 4 shows the WTMAD-2 values of r²SCAN calculated on self-consistent and HF densities, categorized by closed/open-shell, spin-contaminated/uncontaminated, and density-insensitive/sensitive. (Other functionals are shown in Figure S3.) Yellow stars indicate the densities chosen by the recommended DC(HF)-DFT scheme, and in most cases, the yellow stars follow the lowest energies. For spin-uncontaminated density-insensitive cases, HF and self-consistent densities show similar performances, as expected. The improvements of the HF density over the self-consistent density for spin-uncontaminated density-sensitive cases also match the previous studies of DC-DFT. ROHF densities clearly reduce the error for the spin-contaminated cases, which shows that the UHF-DFT error in the region is due to the spin-contamination of the UHF wave function.

We stress this does *not* mean that (a) ROHF gives better energetics than UHF, (b) breaking of symmetries in self-consistent DFT calculations is good or bad, or (c) ROHF spindensities are somehow "better" than those of UHF. All it means is that ROHF densities yield better energetics than UHF densities when several approximate functions are evaluated on those spin densities for spin-contaminated systems.

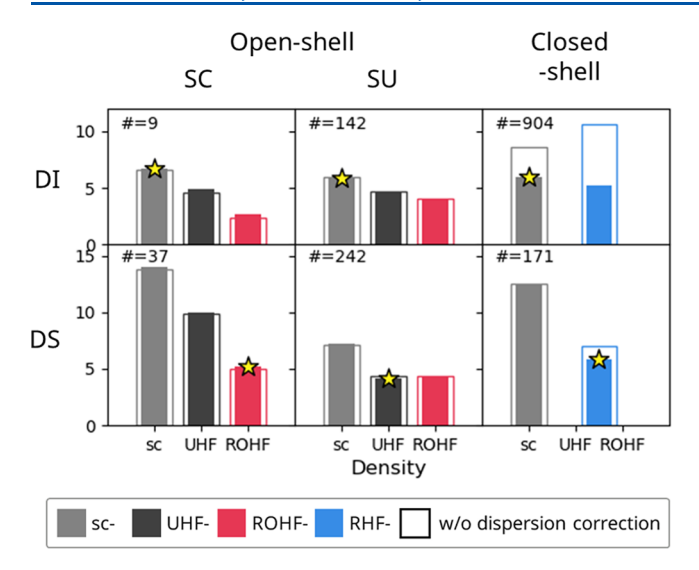


Figure 4. The weighted total mean absolute deviations (WTMAD-2, kcal/mol) of r²SCAN for reactions in GMTKN55 grouped by open/closed-shell, spin-contaminated/uncontaminated (SC/SU), and density-insensitive/sensitive (DI/DS). The number of reactions included in each group is also shown. Gray/blue/black/red bars indicate self-consistent (sc-)/RHF-/UHF-/ROHF-r²SCAN, and filled/empty bars are with/without dispersion correction, D4 for self-consistent DFT and DC4 for HF-DFT. Yellow stars denote DC(HF)-DFT-DC4 chosen for each group according to the suggested recipe (seeFigure S3 for other functionals).

In general, it has been recommended to use the HF density only when reactions are density-sensitive, but when dispersion corrections (fit correctly following the scope of DC-DFT) are included, using the HF densities always yields the best performance. Among these particular examples shown in Figures 3 and 4, r²SCAN-DC4 with ROHF density was shown to be the best in all six categories. Therefore, one could always use ROHF density for this case, but with a caveat. For spincontaminated and density-insensitive cases, the WTMAD-2 error reduction is noticeable when using ROHF densities, but this is due to the inclusion of many reactions with relatively small reference energies and, therefore, large weights in the WTMAD-2 scheme, such as the radical stabilization energy subset (RSE43). The MAE difference between self-consistent and UHF/ROHF densities is smaller than 1.4 kcal/mol. Further study may yet yield better densities, but the ROHF density is a practical remedy for spin contamination at present.

In summary, our study highlights the importance of considering spin contamination in open-shell HF-DFT calculations. HF-DFT has received a lot of attention recently due to its cost-effective nature and significant energetic improvements in DFT calculations. The method involves calculating DFT energies on HF densities instead of their self-consistent ones. Based on this success, HF-r²SCAN-DC4 has been developed and has shown remarkable performance in challenging systems like water. However, previous performance studies of HF-DFT have avoided the issue of spin contamination. For example, it was briefly discussed in the context of DC(HF)-DFT that HF-DFT should only be applied where density sensitivity is high and spin contamination is low.²

We have provided performance studies of two different open-shell HF densities by using various density functional approximations. For spin-contaminated cases, ROHF densities reduced WTMAD-2 errors relative to self-consistent densities for all three types of functionals, including GGA, mGGA, and hybrid, while giving an only slightly higher WTMAD-2 in uncontaminated cases. The double-hybrid HF-DFT functional BL1p suffered most severely from spin contamination in UHF. While the two HF densities showed similar performance in open-shell spin-uncontaminated cases, treating the spin contamination by using ROHF densities showed clear improvements in spin-contaminated cases, with WTMAD-2 values varying from 25 kcal/mol for UBL1p to 5 kcal/mol for ROBL1p. Even for the less pronounced HF-r²SCAN-DC4, ROHF densities reduced the spin-contaminated WTMAD-2 by about a factor of 2 relative to UHF densities. These results highlight the importance of considering spin contamination in open-shell HF-DFT calculations.

Furthermore, in conjunction with the DC(HF)-DFT concept, we emphasize the need for caution when applying DC-DFT in systems with spin contamination. We also offer guidance on handling open-shell systems, as discussed in Figure 4. We have elucidated the criteria governing the process conditions (i.e., density-sensitive if $\tilde{S}>2$ kcal/mol and spin-contaminated if $\Delta \langle \hat{S}^2 \rangle > 0.1)$, parametrized the DC4 correction, and evaluated the performance of two additional popular functionals, PBE and PBE0, which exhibited trends similar to the functionals discussed in the main text (refer to the Supporting Information). Our goal of this work is to expand the applicability of DC-DFT to a broader spectrum of systems while providing valuable insights into open-shell computations.

COMPUTATIONAL DETAILS

The GMTKN55 database includes 5 subsets, and the details are presented in Table S2. All reference energies, geometries of systems, and self-consistent DFT results except for self-consistent r²SCAN are from ref 48.

Reactions that contain one or more open-shell systems are marked as open-shell or otherwise closed-shell. For open-shell reactions, all of the constituent components are calculated with the same HF method. That is, we do not mix UHF and ROHF densities in one reaction. We define $\Delta \langle \hat{S}^2 \rangle$ of a case (reaction or energy difference) by the highest $\Delta \langle \hat{S}^2 \rangle$ value among all constituent components and density sensitivity \tilde{S} by eq 4 where \tilde{E} is the corresponding energy difference. In closed-shell systems, all HF calculations are carried out using the restricted form (RHF), which has no bearing on the open-shell HF comparison.

Each case is classified as density-sensitive/insensitive and spin-contaminated/uncontaminated. We label a reaction as spin-contaminated if its $\Delta \langle \hat{S}^2 \rangle > 0.1$, and spin-uncontaminated otherwise. For density sensitivity, we follow the criteria of Sim et al. to label a reaction as density sensitive if $\tilde{S} > 2$ kcal/mol, otherwise density insensitive. Density sensitivity values depend on functionals, so the number of reactions included in density-sensitive or -insensitive groups is different.

All HF and DFT calculations are performed via the Python-based Simulations of Chemistry Framework, ⁵⁰ utilizing customized Python codes for CUHF. The Ahlrichs def2-QZVPPD basis set ^{51,52} was used for all calculations. The methods analyzed are the self-consistent-/UHF-/ROHF-DFT with 4 generalized gradient approximations (GGAs) (BLYP, ^{53–55} RPBE, ⁵⁶ PW91, ⁵⁷ and PBE, ⁵⁸), 4 meta-GGAs

(TPSS, 59 M06L, 60 SCAN, 61 and $\rm r^2SCAN^{62}$), 5 hybrids (B3LYP, 63,64 TPSSh, 65 PBE0, 66,67 M06, 68 and M06-2X 68), and two fully HF-DFT methods HF-r^2SCAN-DC4 8 and BL1p. 19

ASSOCIATED CONTENT

Supporting Information

The Supporting Information is available free of charge at https://pubs.acs.org/doi/10.1021/acs.jpclett.3c02017.

Numbers of open-shell/spin-contaminated reactions contained in each category of GMTKN55 and the definition of WTMAD-2, D4/DC4 parameters and descriptions about HF-r²SCAN-DC4, $\Delta \langle \hat{S}^2 \rangle$ criterion scan results, BL1p description and α parameter scan results, and Figure 4 for other functionals (PDF)

Raw data of all calculations performed in this work (ZIP)

Transparent Peer Review report available (PDF)

AUTHOR INFORMATION

Corresponding Author

Eunji Sim — Department of Chemistry, Yonsei University, Seoul 03722, Korea; ⊙ orcid.org/0000-0002-4139-0960; Email: esim@yonsei.ac.kr

Authors

Hayoung Yu — Department of Chemistry, Yonsei University, Seoul 03722, Korea; orcid.org/0000-0003-3272-6503

Suhwan Song — Department of Chemistry, Yonsei University, Seoul 03722, Korea; orcid.org/0000-0002-7768-6181

Seungsoo Nam — Department of Chemistry, Yonsei University, Seoul 03722, Korea; orcid.org/0000-0001-9948-6140

Kieron Burke — Department of Chemistry, University of California, Irvine, California 92697, United States; orcid.org/0000-0002-6159-0054

Complete contact information is available at: https://pubs.acs.org/10.1021/acs.jpclett.3c02017

Notes

The authors declare no competing financial interest.

ACKNOWLEDGMENTS

We are grateful for support from the National Research Foundation of Korea (NRF-2020R1A2C2007468) and Korea Environment Industry & Technology Institute (KEITI) through "Advanced Technology Development Project for Predicting and Preventing Chemical Accidents" Program funded by Korea Ministry of Environment (MOE) (RS-2023-00219144). K.B. acknowledges support from NSF grant No.CHE-2154371.

REFERENCES

- (1) Kim, M.-C.; Sim, E.; Burke, K. Understanding and reducing errors in density functional calculations. *Phys. Rev. Lett.* **2013**, *111*, 073003.
- (2) Song, S.; Vuckovic, S.; Sim, E.; Burke, K. Density-corrected dft explained: Questions and answers. *J. Chem. Theory Comput.* **2022**, *18*, 817–827.
- (3) Sim, E.; Song, S.; Vuckovic, S.; Burke, K. Improving results by improving densities: Density-corrected density functional theory. *J. Am. Chem. Soc.* **2022**, 144, 6625–6639.

- (4) Nam, S.; Song, S.; Sim, E.; Burke, K. Measuring density-driven errors using kohn—sham inversion. *J. Chem. Theory Comput.* **2020**, *16*, 5014—5023.
- (5) Theoretical and Computational Chemistry Laboratory; Yonsei University. DC-DFT. https://tccl.yonsei.ac.kr/. (Accessed: 2023-09-04).
- (6) Dasgupta, S.; Lambros, E.; Perdew, J. P.; Paesani, F. Elevating density functional theory to chemical accuracy for water simulations through a density-corrected many-body formalism. *Nat. Commun.* **2021**, *12*, 6359.
- (7) Dasgupta, S.; Shahi, C.; Bhetwal, P.; Perdew, J. P.; Paesani, F. How good is the density-corrected scan functional for neutral and ionic aqueous systems, and what is so right about the hartree—fock density? *J. Chem. Theory Comput.* **2022**, *18*, 4745–4761.
- (8) Song, S.; Vuckovic, S.; Kim, Y.; Yu, H.; Sim, E.; Burke, K. Extending density functional theory with near chemical accuracy beyond pure water. *Nat. Commun.* **2023**, *14*, 799.
- (9) Rana, B.; Coons, M. P.; Herbert, J. M. Detection and correction of delocalization errors for electron and hole polarons using density-corrected dft. *J. Phys. Chem. Lett.* **2022**, *13*, 5275–5284.
- (10) Rana, B.; Beran, G. J.; Herbert, J. M. Correcting π -delocalisation errors in conformational energies using density-corrected dft, with application to crystal polymorphs. *Mol. Phys.* **2023**, *121*, e2138789.
- (11) Santra, G.; Martin, J. M. What types of chemical problems benefit from density-corrected dft? a probe using an extensive and chemically diverse test suite. *J. Chem. Theory Comput.* **2021**, 17, 1368–1379.
- (12) Nam, S.; Cho, E.; Sim, E.; Burke, K. Explaining and fixing dft failures for torsional barriers. *J. Phys. Chem. Lett.* **2021**, *12*, 2796–2804.
- (13) Kim, M.-C.; Sim, E.; Burke, K. Communication: Avoiding unbound anions in density functional calculations. *J. Chem. Phys.* **2011**, *134*, 171103.
- (14) Kim, M.-C.; Park, H.; Son, S.; Sim, E.; Burke, K. Improved dft potential energy surfaces via improved densities. *J. Phys. Chem. Lett.* **2015**, *6*, 3802–3807.
- (15) Kim, M.-C.; Sim, E.; Burke, K. Ions in solution: Density corrected density functional theory (dc-dft). *J. Chem. Phys.* **2014**, *140*, 18A528.
- (16) Song, S.; Kim, M.-C.; Sim, E.; Benali, A.; Heinonen, O.; Burke, K. Benchmarks and reliable dft results for spin gaps of small ligand fe (ii) complexes. *J. Chem. Theory Comput.* **2018**, *14*, 2304–2311.
- (17) Kim, Y.; Song, S.; Sim, E.; Burke, K. Halogen and chalcogen binding dominated by density-driven errors. *J. Phys. Chem. Lett.* **2019**, *10*, 295–301.
- (18) Morgante, P.; Autschbach, J. Density-corrected density functional theory for molecular properties. *J. Phys. Chem. Lett.* **2023**, 14, 4983–4989.
- (19) Song, S.; Vuckovic, S.; Sim, E.; Burke, K. Density sensitivity of empirical functionals. *J. Phys. Chem. Lett.* **2021**, *12*, 800–807.
- (20) Montoya, A.; Truong, T. N.; Sarofim, A. F. Spin contamination in hartree-fock and density functional theory wavefunctions in modeling of adsorption on graphite. *J. Phys. Chem. A* **2000**, *104*, 6108–6110.
- (21) Bryenton, K. R.; Adeleke, A. A.; Dale, S. G.; Johnson, E. R. Delocalization error: The greatest outstanding challenge in density-functional theory. *Wiley Interdiscip. Rev.: Comput. Mol. Sci.* **2023**, *13*, e1631
- (22) Gräfenstein, J.; Kraka, E.; Filatov, M.; Cremer, D. Can unrestricted density-functional theory describe open shell singlet biradicals? *Int. J. Mol. Sci.* **2002**, *3*, 360–394.
- (23) Shahidi, F.; Janitha, P.; Wanasundara, P. Phenolic antioxidants. *Crit. Rev. Food Sci. Nutr.* **1992**, *32*, *67*–103.
- (24) Zeb, A. Concept, mechanism, and applications of phenolic antioxidants in foods. *J. Food Biochem.* **2020**, 44, e13394.
- (25) Orlando, J. J.; Tyndall, G. S.; Vereecken, L.; Peeters, J. The atmospheric chemistry of the acetonoxy radical. *J. Phys. Chem. A* **2000**, *104*, 11578–11588.

- (26) Crisostomo, S.; Pederson, R.; Kozlowski, J.; Kalita, B.; Cancio, A. C.; Datchev, K.; Wasserman, A.; Song, S.; Burke, K. Seven useful questions in density functional theory. *Lett. Math. Phys.* **2023**, *113*, 42.
- (27) Martín-Fernández, C.; Harvey, J. N. On the use of normalized metrics for density sensitivity analysis in dft. *J. Phys. Chem. A* **2021**, 125, 4639–4652.
- (28) Graf, D.; Thom, A. J. A simple and efficient route towards improved energetics within the framework of density-corrected density functional theory. *arXiv* 2023, 2304.04473.
- (29) Schlegel, H. B. Spin contamination. *Encycl. Comput. Chem.* **1998**. 4. DOI: 10.1002/0470845015.csa020
- (30) Williams, T. G.; DeYonker, N. J.; Ho, B. S.; Wilson, A. K. The correlation consistent composite approach: the spin contamination effect on an mp2-based composite methodology. *Chem. Phys. Lett.* **2011**, *504*, 88–94.
- (31) Andrews, J. S.; Jayatilaka, D.; Bone, R. G.; Handy, N. C.; Amos, R. D. Spin contamination in single-determinant wavefunctions. *Chem. Phys. Lett.* **1991**, *183*, 423–431.
- (32) Menon, A. S.; Radom, L. Consequences of spin contamination in unrestricted calculations on open-shell species: Effect of hartree-fock and møller- plesset contributions in hybrid and double-hybrid density functional theory approaches. *J. Phys. Chem. A* **2008**, *112*, 13225–13230.
- (33) Goodpaster, J. D.; Barnes, T. A.; Manby, F. R.; Miller, T. F. Density functional theory embedding for correlated wavefunctions: Improved methods for open-shell systems and transition metal complexes. *J. Chem. Phys.* **2012**, *137*, 224113 DOI: 10.1063/1.4770226.
- (34) Yang, B.; Wang, S.; Wang, L. Rapid gas-phase autoxidation of nicotine in the atmosphere. *J. Phys. Chem. A* **2022**, *126*, 6495–6501.
- (35) Baker, J.; Scheiner, A.; Andzelm, J. Spin contamination in density functional theory. *Chem. Phys. Lett.* **1993**, *216*, 380–388.
- (36) Perdew, J. P.; Savin, A.; Burke, K. Escaping the symmetry dilemma through a pair-density interpretation of spin-density functional theory. *Phys. Rev. A* **1995**, *51*, 4531.
- (37) Zunger, A.; Malyi, O. I. Understanding doping of quantum materials. *Chem. Rev.* **2021**, *121*, 3031–3060.
- (38) Perdew, J. P.; Chowdhury, S. T. u. R.; Shahi, C.; Kaplan, A. D.; Song, D.; Bylaska, E. J. Symmetry breaking with the scan density functional describes strong correlation in the singlet carbon dimer. *J. Phys. Chem. A* **2023**, *127*, 384–389.
- (39) Jensen, F. 4.8.2. Unrestricted and projected Møller-Plesset methods; John Wiley & Sons, 2nd ed., 2007; p 168.
- (40) Plakhutin, B.; Gorelik, E.; Breslavskaya, N. Koopmans' theorem in the rohf method: Canonical form for the hartree-fock hamiltonian. *J. Chem. Phys.* **2006**, *125*, 204110.
- (41) Baker, J. An investigation of the annihilated unrestricted hartree—fock wave function and its use in second-order mo/ller—plesset perturbation theory. *J. Chem. Phys.* **1989**, *91*, 1789–1795.
- (42) Amos, A.; Hall, G. Single determinant wave functions. Proceedings of the Royal Society of London. Series A. Mathematical and Physical Sciences 1961, 263, 483–493.
- (43) Tsuchimochi, T.; Scuseria, G. E. Communication: Rohf theory made simple. *J. Chem. Phys.* **2010**, *133*, 141102.
- (44) Tsuchimochi, T.; Scuseria, G. E. Constrained active space unrestricted mean-field methods for controlling spin-contamination. *J. Chem. Phys.* **2011**, *134*, 064101.
- (45) Rettig, A.; Hait, D.; Bertels, L. W.; Head-Gordon, M. Third-order møller-plesset theory made more useful? the role of density functional theory orbitals. *J. Chem. Theory Comput.* **2020**, *16*, 7473–7489.
- (46) Goerigk, L.; Hansen, A.; Bauer, C.; Ehrlich, S.; Najibi, A.; Grimme, S. A look at the density functional theory zoo with the advanced gmtkn55 database for general main group thermochemistry, kinetics and noncovalent interactions. *Phys. Chem. Chem. Phys.* **2017**, 19, 32184–32215.
- (47) Caldeweyher, E.; Ehlert, S.; Hansen, A.; Neugebauer, H.; Spicher, S.; Bannwarth, C.; Grimme, S. A generally applicable atomic-

- charge dependent london dispersion correction. J. Chem. Phys. 2019, 150, 154122.
- (48) Reckien, W. *Gmtkn55*. 2017. URL https://www.chemie.unibonn.de/grimme/de/software/gmtkn/gmtkn. (Accessed: 2023-09-03).
- (49) Sim, E.; Song, S.; Burke, K. Quantifying density errors in dft. J. Phys. Chem. Lett. 2018, 9, 6385–6392.
- (50) Sun, Q.; Berkelbach, T. C.; Blunt, N. S.; Booth, G. H.; Guo, S.; Li, Z.; Liu, J.; McClain, J. D.; Sayfutyarova, E. R.; Sharma, S.; et al. Pyscf: the python-based simulations of chemistry framework. *Wiley Interdiscip. Rev.: Comput. Mol. Sci.* **2018**, *8*, e1340.
- (51) Weigend, F.; Ahlrichs, R. Balanced basis sets of split valence, triple zeta valence and quadruple zeta valence quality for h to rn: Design and assessment of accuracy. *Phys. Chem. Chem. Phys.* **2005**, *7*, 3297–3305.
- (52) Rappoport, D.; Furche, F. Property-optimized gaussian basis sets for molecular response calculations. *J. Chem. Phys.* **2010**, *133*, 134105.
- (53) Becke, A. D. Density-functional exchange-energy approximation with correct asymptotic behavior. *Phys. Rev. A* **1988**, *38*, 3098.
- (54) Lee, C.; Yang, W.; Parr, R. G. Development of the colle-salvetti correlation-energy formula into a functional of the electron density. *Phys. Rev. B* **1988**, *37*, 785.
- (55) Miehlich, B.; Savin, A.; Stoll, H.; Preuss, H. Results obtained with the correlation energy density functionals of becke and lee, yang and parr. *Chem. Phys. Lett.* **1989**, *157*, 200–206.
- (56) Hammer, B.; Hansen, L. B.; Nørskov, J. K. Improved adsorption energetics within density-functional theory using revised perdew-burke-ernzerhof functionals. *Phys. Rev. B* **1999**, *59*, 7413.
- (57) Wang, Y.; Perdew, J. P. Correlation hole of the spin-polarized electron gas, with exact small-wave-vector and high-density scaling. *Phys. Rev. B* **1991**, *44*, 13298.
- (58) Perdew, J. P.; Burke, K.; Ernzerhof, M. Generalized gradient approximation made simple. *Phys. Rev. Lett.* **1996**, *77*, 3865.
- (59) Tao, J.; Perdew, J. P.; Staroverov, V. N.; Scuseria, G. E. Climbing the density functional ladder: Nonempirical metageneralized gradient approximation designed for molecules and solids. *Phys. Rev. Lett.* **2003**, *91*, 146401.
- (60) Zhao, Y.; Truhlar, D. G. A new local density functional for main-group thermochemistry, transition metal bonding, thermochemical kinetics, and noncovalent interactions. *J. Chem. Phys.* **2006**, *125*, 194101.
- (61) Sun, J.; Ruzsinszky, A.; Perdew, J. P. Strongly constrained and appropriately normed semilocal density functional. *Phys. Rev. Lett.* **2015**, *115*, 036402.
- (62) Furness, J. W.; Kaplan, A. D.; Ning, J.; Perdew, J. P.; Sun, J. Accurate and numerically efficient r2scan meta-generalized gradient approximation. *J. Phys. Chem. Lett.* **2020**, *11*, 8208–8215.
- (63) Becke, A. D. A new mixing of hartree–fock and local density-functional theories. *J. Chem. Phys.* **1993**, 98, 1372–1377.
- (64) Stephens, P. J.; Devlin, F. J.; Chabalowski, C. F.; Frisch, M. J. Ab initio calculation of vibrational absorption and circular dichroism spectra using density functional force fields. *J. Phys. Chem.* **1994**, 98, 11623–11627.
- (65) Staroverov, V. N.; Scuseria, G. E.; Tao, J.; Perdew, J. P. Comparative assessment of a new nonempirical density functional: Molecules and hydrogen-bonded complexes. *J. Chem. Phys.* **2003**, *119*, 12129–12137.
- (66) Adamo, C.; Barone, V. Toward reliable density functional methods without adjustable parameters: The pbe0 model. *J. Chem. Phys.* **1999**, *110*, 6158–6170.
- (67) Ernzerhof, M.; Scuseria, G. E. Assessment of the perdewburke-ernzerhof exchange-correlation functional. *J. Chem. Phys.* **1999**, *110*, 5029–5036.
- (68) Zhao, Y.; Truhlar, D. G. The m06 suite of density functionals for main group thermochemistry, thermochemical kinetics, non-covalent interactions, excited states, and transition elements: two new functionals and systematic testing of four m06-class functionals and 12 other functionals. *Theor. Chem. Acc.* 2008, 120, 215–241.